Journal of Visualization, Vol. 3, No. 2 (2000) 157-164

PIV Measurements of the Flow and Turbulent Characteristics of a Round Jet in Crossflow

Kim, K. C.,* Kim, S. K.* and Yoon, S. Y.*

* School of Mechanical Engineering, Pusan National University, Pusan, 609-735, Korea

Received 7 January 2000.
Revised 2 May 2000.

***Abstract*:** The instantaneous and ensemble averaged flow characteristics of a round jet issuing normally into a crossflow was studied using a flow visualization technique and Particle Image Velocimetry measurements. Experiments were performed at a jet-to-crossflow velocity ratio, 3.3 and two Reynolds numbers, 1,050 and 2,100, based on crossflow velocity and jet diameter. Instantaneous laser tomographic images of the vertical center plane of the crossflow jet show that there exists very different natures in the flow structures of the near field jet due to Reynolds number effect even though the velocity ratio is same. It is found that the shear layer becomes much thicker when the Reynolds number is 2,100 because of the strong entrainment of the inviscid fluid by turbulent interaction between the jet and crossflow. The mean and second order statistics are calculated by ensemble averaging over 1,000 realizations of instantaneous velocity fields. The detail characteristics of mean flow field, streamwise and vertical rms velocity fluctuations, and Reynolds shear stress distributions are presented. The new PIV results are compared with those from previous experimental and LES studies.

***Keywords*:** crossflow jet, particle image velocimetry, Reynolds number dependency, flow and turbulence characteristics.

1. Introduction

The jet in crossflow(JICF) is one of the most complex turbulent flow, but it seems to be a canonical form of many industrial and/or environmental engineering problems. The fundamental behavior of a nonbuoyant turbulent round jet issuing normally into a wall boundary layer is essential for understanding pollutant dispersion from stacks, designing V/STOL aircraft and providing injection cooling of gas turbine combustor walls. Many experimental and numerical investigations of the JICF have been carried out and a thorough review of JICF has been conducted by Margason(1993).

Early stages of experimental work centered around measuring the jet trajectory for different combinations of flow parameters as performed by Pratte and Baines(1967). Later research began to collect mean velocity and turbulence statistics data using hot wires and laser Doppler velocimetry done by Crabb, Durao and Whitelaw(1981). Andreopoulos and Rodi(1984) used a triple wire probe to measure all three components of velocity simultaneously. Fric and Roshko(1994) suggested that the key features of vortical structures associated in the JICF are the horseshoe vortices in front of the jet, the shear layer vortices at the edge of the jet, the vertically oriented vortices which connect the jet body with wall boundary layer in the wake region, and the counter-rotating vortex pair(CVP) which is often observed in the far-field aligned with the trajectory of the jet. Kelso, Lim and Perry(1996) investigated detail nature of the jet structure employing dye tracer in a water tunnel and flying hot wires in a wind tunnel. They argued that the initial vortical roll up of the jet shear layer initiates the downstream development of the CVP through a vortex breakdown mechanism. Kim and Shin(1998) froze the vertical

centerplane of the jet flow using laser tomographic method and found that the Kelvin-Helmholtz type roll up structures are appeared both upstream and downstream boundaries of the JICF. Recently, Yuan, Street and Ferziger(1999, here after YSF) carried out the LES of a round jet in crossflow. Their simulations reproduced large scale, coherent structures observed in experimental flow visualizations and the mean and turbulent statistics computed from the simulations were reasonably matched with experimental measurements.

In spite of numerous studies for the JICF have performed, many questions are remained still unanswered. Many investigators seem to agree that the original source of the CVP in the jet shear layer, but the means by which this vorticity realigns to produce CVP is still unclean. The effect of flow parameters on the evolution of vortical motions in the JICF should be scrutinized in detail. To verify the predicted results from LES method, more accurate and plentiful experimental data are needed.

The objective of present study is providing accurate instantaneous and averaged velocity fields in the vertical centerplane of a jet in crossflow using a PIV method. The effects of Reynolds number on the jet development are also examined. We compare PIV measurements with LES results and previous experimental data.

2. Experimental Apparatus and Method

Flow visualization and flow field measurements were made in a small open type low speed wind tunnel. The tunnel has a working section measuring 30 cm height, 80 cm width and 200 cm in length. The test section walls are made of plexiglass and glass plates. The air driven by a variable speed 3 hp centrifugal fan passes a settling chamber, a 2.67:1 area ratio contraction, then enters to the test section through a fine mesh screen. The freestream turbulence intensity at the entrance of the test section is about 1%.

The round jet is issued normally into the test section from a 16 mm inner diameter nozzle pipe which is mounted at the bottom plate of the wind tunnel 25 cm downstream from the exit of the contraction nozzle. The jet is generated by air compressor then passes through a mixing chamber, a pressure regulator and a flowmeter. Olive oil aerosol particles whose diameter are 2 μm in average produced by a Laskin nozzle were supplied into the mixing chamber. A straight pipe of 35 cm in length is connected from the mixing chamber to the jet exit at the test section bottom plate.

The most dominant parameter which governs flow characteristics of the JICF is the momentum ratio between the jet and the crossflow. If the two flows have the same density, the momentum ratio turns out to be the velocity ratio R as following:

$$R = V_j/U_\infty$$

where, V_j equals to the flow rate divided by the jet cross section area and U_∞ denotes the free stream velocity. We fixed the velocity ratio R as 3.3 in this experiment. At the same velocity ratio conditions, Reynolds number may play a key role in the flow behavior. We performed experiments with two Reynolds numbers, 1,050 and 2,100 based on crossflow velocity and jet diameter. These Reynolds numbers are the same as YSF(1999) carried out LES of the JICF. The corresponding freestream velocities are 1.0 m/s and 2.0 m/s, respectively. We did not use a tripping wire, so that the approaching boundary layers are considered to be laminar boundary layers with initial boundary layer heights of 12 mm and 10 mm at the position of the hole, respectively. The incoming pipe flow Reynolds numbers are 3,470 and 6,940 based on the average velocity V_j and the pipe inner diameter.

Flow visualization study was conducted before the main PIV experiment. To obtain instantaneous tomographic image of the JICF, a laser sheet beam having less than 1 mm thickness was illuminated during 4 ns using a 200 mJ/pulse Nd:Yag laser. The olive oil aerosols were supplied only into the jet flow, hence the frozen jet flow patterns are clearly recognized as the scattering image.

Two dimensional velocity vector fields at the vertical centerplane were measured using an Nd:Yag based PIV system. The schematic diagram of the PIV setup and the coordinate system is appeared in Fig. 1. The online PIV system being used in this study consists of a dual pulse Nd:Yag laser system, a synchronizer(TSI, 610032), a 1K by 1K high resolution CCD camera and a Pentium computer to control the system. We put a standard Nikon 50 mm lens in front of the CCD camera to prevent the image distortion error. The olive oil particles were supplied into both wind tunnel and pipe. The uniformity of the particle distribution and the intensity of the scattered light have been checked before experiment.

The interrogation of the velocity vector was carried out using INSIGHT-NT software adopting two frame cross-correlation method. A total of 16,002 velocity vectors are interrogated, hence the spatial resolution of the

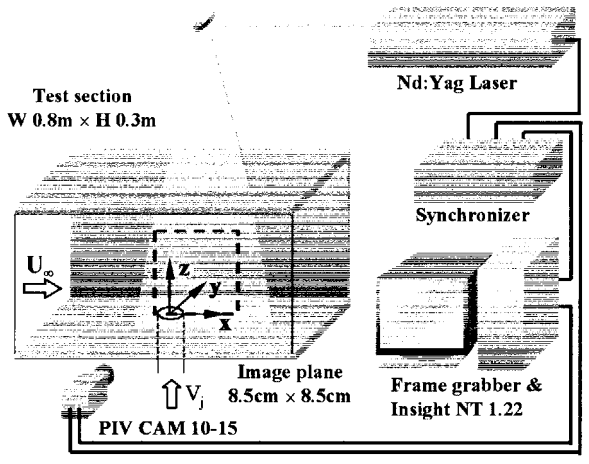

Fig. 1. Schematic diagram of experimental setup.

velocity data is 0.63 mm. In order to determine the maximum cross-correlation coefficients, we select the size of an interrogation window as 16×16 pixels and 50% of overlap was permitted. Using the post processing software being developed in our laboratory, we eliminated bad vectors and accomplished various statistical calculations including velocity gradient estimates.

3. Results and Discussions

Figures 2 and 3 show the instantaneous flow patterns of JICF taken at the jet centerplane when the Reynolds numbers are 1,050 and 2,100, respectively. Note that the velocity ratio for each cases are equally 3.3. Very well organized Kelvin-Helmholtz type vortex roll-up phenomena occur at both upstream and downstream side of the jet shear layer. Kim and Shin(1998) observed the same roller structures from their laser tomographic images taken at the Reynolds number of 710 with the velocity ratio of 3.0. One more coherent roll-up at the upper edge of the jet can be seen in the present study compared with the Kim and Shin(1998)'s results before the abrupt vortex breakdown. It is conjectured that the higher Reynolds number, the faster vortex shedding.

Fig. 2. Instantaneous tomography image at the centerplane, Re_D = 1,050.

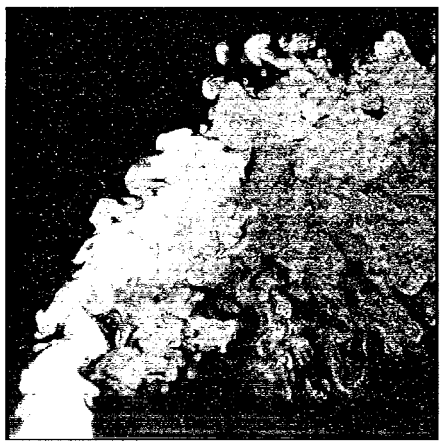

Fig. 3. Instantaneous tomography image at the centerplane, Re_D = 2,100.

The most striking nature of JICF is that the instantaneous flow pattern of the higher Reynolds number shows quite different structures as shown in Fig. 3. The jet depicts highly turbulent motions from the beginning of the JICF. The spanwise rollers are found on the upstream and downstream edges, but less regularly formed than those of the Re_D = 1,050 case. If we remember that the velocity ratios are same for both cases, the Reynolds number plays dominant role in the momentum transport of the JICF. It is clear that there exists a critical Reynolds

number between 1,050 and 2,100 when the velocity ratio is given 3.3. The wide spread of white region in Fig. 3 indicates the strong mixing of two fluids due to turbulent interactions.

At z/D = 2.0 in Fig. 3, the rollers formed the upstream and downstream shear layers, which have opposite signs, interact in an unpredictable manner, creating gaps in the jet flow. YSF observed this behavior from their LES results which have the same velocity ratio and Reynolds number with the present experiment. The gaps produced by these vortex interactions on the upstream edge of the jet prove to be an important mechanism for entrainment of crossflow fluid by the jet.

Figures 4 and 5 illustrate the instantaneous velocity vector fields at the jet centerplane for the case of Reynolds number 1,050 and 2,100, respectively. As observed from the tomographic images, the regular vortical motions are vividly shown at the upstream edge of the jet in the case of Re_D = 1,050. The shear layer vortices disappear suddenly when the jet bents over to the downstream. The spanwise rollers are strong, energetic structures which penetrate deeply into the crossflow. The stability of the initial jet shear layers may explain the strong Re_D dependence we observed in the instantaneous flow patterns. The onset of instability and the subsequent vortical roll-up occur later in the trajectory of the lower Re_D jet. The roll-up is produced by the lower Re_D jet then penetrate more deeply into the crossflow.

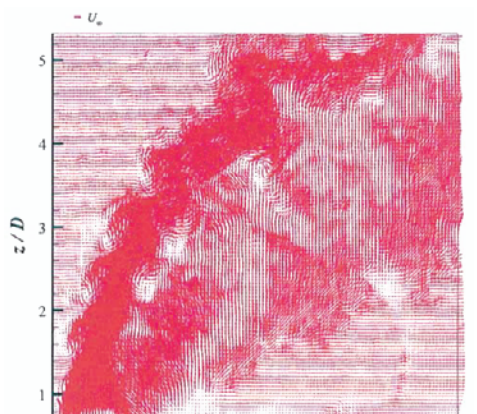

Fig. 4. Instantaneous velocity vector field at the centerplane, Re_D = 1,050.

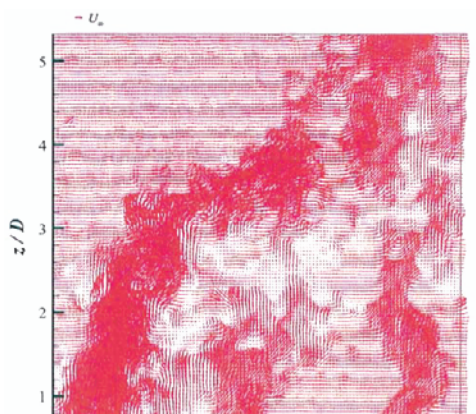

Fig. 5. Instantaneous velocity vector field at the centerplane, Re_D = 2,100.

The velocity field at the downstream region of the jet which is not clear in the tomographic image demonstrates many interesting phenomena. Due to the negative pressure formed at backside of the jet column, large amount of reverse flow vectors are observed in both Reynolds number cases. Kelso, Lim and Perry(1996) observed that tube-like structures began on the lateral edges of the jet. These tubes, one on each side of the jet, extended around the jet body and then up along the back side of the jet, roughly matching the jet trajectory. They proposed that vorticity found in these tubes contributed to the circulation of the CVP. We can see the evidence of these structures from Figs. 4 and 5, in which active vertical velocity components can be seen at the downstream region. Near the wake region at the downstream side, intermittent velocity vector packets are appeared. We hypothesize that the nature comes from upright vortices in the wake region.

Time averaged velocity fields are obtained by ensemble mean using 1,000 instantaneous velocity fields. Each realization needs two continuous particle images, so that total 2,000 image files are used for averaging. We accomplished a statistical test for the mean velocity and the second order turbulence quantities. The maximum random errors were found to be less than 1% when the ensemble number was greater than 300 for mean veoclity and 600 for $\langle uu \rangle$. Relatively highest deviation was observed in Reynolds shear stress, $\langle uw \rangle$ which showed maximum 3% difference between 1,000 times averaging and 900 times case.

Figures 6 and 7 are the streamline patterns from two-dimensional velocities at Re_D = 1,050 and 2,100, respectively. There are three distinct characteristics of mean velocity field: the main jet flow which comes from nozzle then bents over downstream, the induced flow which starts from backside of the jet accompanying with CVP motion, and the entrained flow which is added to the main flow from adjacent crossflow. The trajectory of the JICF can be defined a streamline which begins at the origin and is indicated as the heavy dashed line in Figs. 6

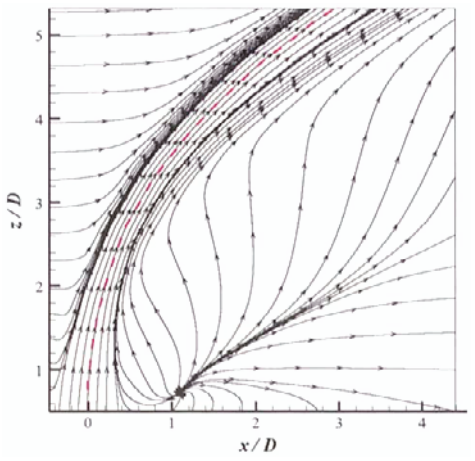

Fig. 6. Streamlines from ensemble averaged velocity field, Re_D = 1,050.

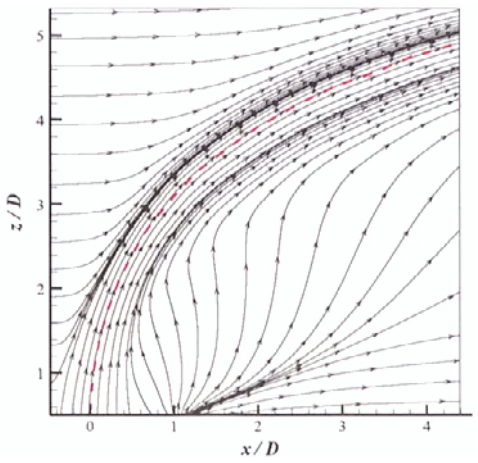

Fig. 7. Streamlines from ensemble averaged velocity field, Re_D = 2,100.

and 7. The trajectory represents the main jet flow but the induced flow and the entrained flow seem to begin a virtual point source.

The effect of Reynolds number is well depicted if we compare the jet trajectories of both cases. The jet bents over quickly when the Reynolds number increases at the given velocity ratio. The difference is noticeable that the lower Reynolds number jet centerline passes about one diameter higher position compared with the higher Reynolds number jet at $x = 3D$ location. It is interesting to note that the nodal points lie at about one diameter downstream from the origin, seems to approach to the wall when the Reynolds number becomes higher. The source locating at x/D = 1.06, z/D = 0.75 for the case of Re_D = 1,050, while the point moves to lower downstream at x/D = 1.13, z/D = 0.5 for the case of Re_D = 2,100. It should be pointed out that there appear vertically oriented streamlines between source points and the wall, which attribute to interact with the JICF and the near wall flow having high vorticity, contributing to generate the upright vortices in the wake region.

To obtain Reynolds stress terms, 1,000 ensemble averaging has done using r.m.s. of the fluctuating velocity field which is subtracting mean velocity from instantaneous velocity field. The results correspond low-pass filtered estimates since we can not resolve the scale less than 0.63 mm. However, it turns out two orders of magnitude smaller than typical large scale eddies so that the Reynolds stresses measured by the present PIV method can be considered highly accurate. The streamwise and vertical components of Reynolds normal stresses are demonstrated in Figs. 8 and 9, respectively.

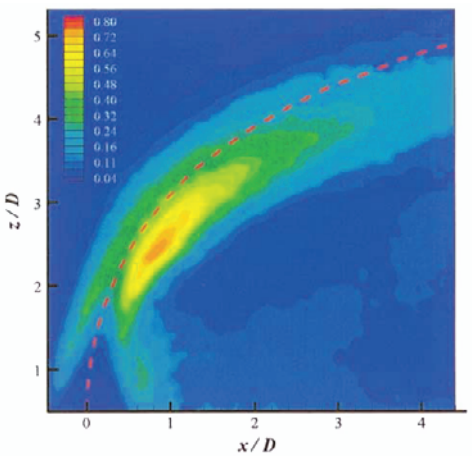

Fig. 8. Contours of streamwise normal stress $<uu>/U_\infty^2$ at the centerplane, Re_D = 2,100.

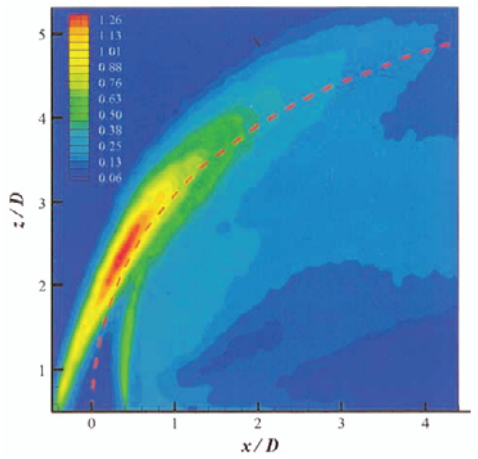

Fig. 9. Contours of vertical normal stress $<ww>/U_\infty^2$ at the centerplane, Re_D = 2,100.

The streamwise velocity fluctuations show small values until one diameter above from the flat plate since fluctuations in the streamwise direction are small in the pipe flow. The roll-up of the jet shear layers starting then the velocity fluctuations then rapidly increased with two rollers merge together. The peak value of the steamwise velocity fluctuation occurs at downstream side with respect to the trajectory near the maximum bent-over location.

The vertical velocity fluctuations develop rather quickly along each side of jet shear layers due to the roll-up processes. Relatively large values in the upstream side shear layer are attributed to the fact that the roll-ups are rapidly produced and well organized in this region. The maximum <*ww*> magnitude is approximately 1.5 times higher than that of <*uu*>. The higher values of <*ww*> are expected as the initial momentum applied by the jet is only in the vertical direction. The location of the <*ww*> maximum lies about 0.5*D* above the <*uu*> maximum. In contrast with <*uu*> maximum, the vertical fluctuation are biased toward the upstream edge of the jet after the rollers meet. One more branch in the <*ww*> contours is observed in downstream of the JICF. This branch can be explained that the <*ww*> production by shear between the jet and the crossflow and by the intermittence of the CVP. From <*uu*> and <*ww*> contours, the turbulence is found to be highly anisotropic at the near field of the JICF.

Figure 10 shows the contour plot of <*uw*>. Again, the spanwise rollers in the near field play the dominant role in Reynolds shear stress production. <*uw*> is strongly negative in the upstream layer and positive in the downstream one where strong horizontal gradients of the vertical velocity are located. After the bent-over, beyond z/D = 3, the negative <*uw*> occurs in the downstream layer due to strong vertical gradients of the horizontal velocity.

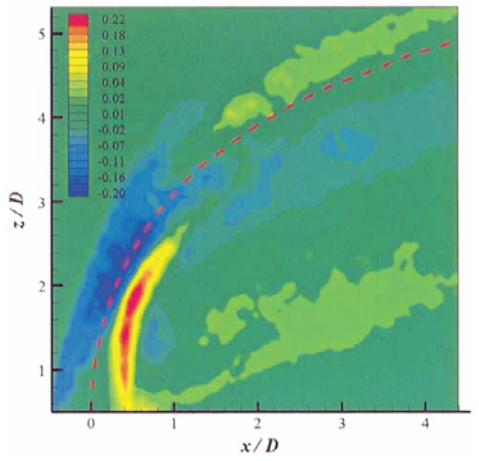

Fig. 10. Contours of Reynolds shear stress $<uw>/U_\infty^2$ at the centerplane, Re_D = 2,100.

To validate our PIV results, we compared our results to the experimental measurements of Sherif and Pletcher(1989) and the LES results performed by YSF. Sherif and Pletcher used a single hot film probe to measure velocity on the centreplane of a JICF with a velocity ratio R = 4.0 and a Reynolds number of 4,820. Since the hot film data could not avoid the cooling by the velocity component along the sensor axis, there should be quite large error especially high intensity region of the Sherif and Pletcher's result. YSF carried out numerical analysis of a JICF with exactly same flow conditions with those of our case but there exist some differences in the approaching boundary layer and the inflow jet condition.

Figure 11 depicts vertical profiles of velocity magnitude on the centerplane at three streamwise locations. The velocity magnitudes were computed by three velocity components in the LES results, while we used two velocity components from the plane PIV results. At x/D = 0.0 location, the agreement of LES and PIV results is quite good. Next two locations, two experimental measurements match well each other, although the peak positions of the hot-film data are lower than those of PIV measurements. It can be explained that the local maxima approach to the wall when the Reynolds number increases. The magnitude and the location of maximum velocity obtained by PIV and LES coincide exactly, but the second peaks computed by LES are higher than experiments. One of the reasons in the difference can be explained that the LES used all three velocity components to estimate the total velocity U_m, while the present experiments could not take into account.

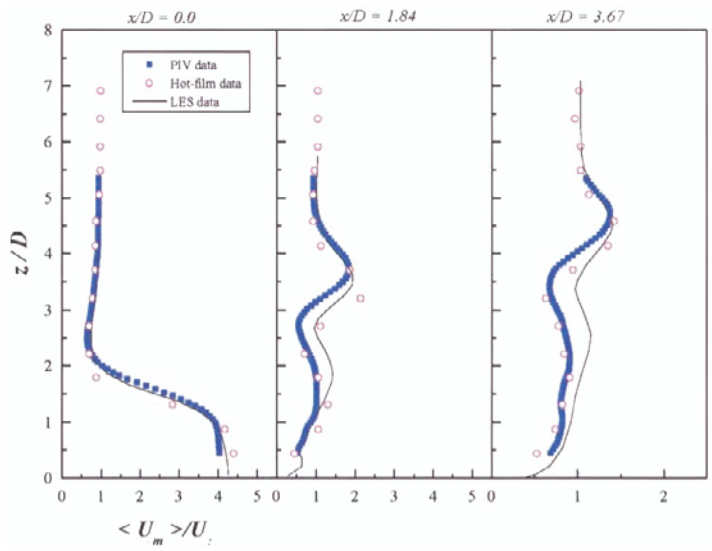

Fig. 11. Comparison of vertical profiles of mean velocity magnitude at the centerplane, Re_D = 2,100.

The r.m.s. fluctuations of velocity magnitude are plotted in Fig. 12. In general, two experimental results agree well than with the LES calculations. At the first station, the excellent agreement between LES and hot-film data comes from intentional adjustment of the incoming jet conditions before simulation. Some of underprediction by LES may be caused from the high mean velocities observed in Fig. 11.

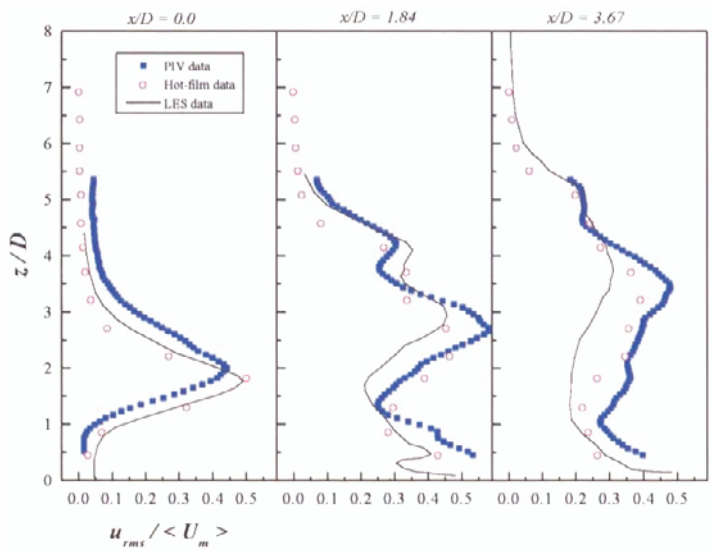

Fig. 12. Comparison of vertical profiles of r.m.s. fluctuations in velocity magnitude at the centerplane, Re_D = 2,100.

4. Conclusions

Instantaneous and ensemble averaged velocity fields in the centerplane of a jet in crossflow have been obtained and compared with the previous experimental and numerical results. It is found that the Reynolds number affects considerably to the development of the jet in crossflow even though at the same velocity ratio. In the case of velocity ratio is 3.3, there exists a critical Reynolds number between 1,050 to 2,100. Above the critical Reynolds number, distinct turbulent nature begins from the jet nozzle while there appears periodical vortex roll-ups both upstream and downstream side of the jet shear layer below the critical Reynolds number. Ensemble averaged mean

velocity field reveals that there are three kinds of characteristic flows named main flow, induced flow and entrained flow which are initiated from counter-rotating vortex formation. Instantaneous velocity field and ensemble averaged turbulence statistics show the spanwise rollers on the upstream and downstream edges of the jet produce intense velocity fluctuations. The jet bents over quickly with the merging of two shear layers, then becomes crossflow. The sign change of Reynolds shear stress at the downstream side of the jet indicates the change of turbulence production mechanism from shear layer vortices to counter rotating motions with the bent-over.

Acknowledgments

This work was supported by the Brain Korea 21 Project, 1999.

References

Andreopoulos, J. and Rodi, W., On the Structure of Jets in Crossflow, J. Fluid Mech., 157 (1984), 163-197.

Crabb, D., Durao, D. F. G. and Whitelaw, J. H., A round jet normal to a crossflow, J. Fluids Engineering, 103 (1981), 142-153.

Fric, T. F. and Roshko, A., Vortical Structure in the Wake of a Transverse Jet, J. Fluid Mech., 279 (1994), 1-147.

Kelso, R. M., Lim, T. T. and Perry, A. E., An Experimental Study of Round Jets in Cross-flow, J. Fluid Mech., 306 (1996), 111-144.

Kim, K. C. and Shin, D. S., A Study on the Topology of Shear Layer Vortex Structure in a Cross Flow Jet Using a Laser Tomographic Visualization Method, 98VSJ-SPIE, AB-057 (1998).

Margason, R. J., Fifty Years of Jet in Crosflow Research, In Computational and Experimental Assessment of Jets in Cross Flow, AGARD-CP-534, Winchester, UK (1993).

Pratte, B. P. and Baines, W. D., Profiles of the Round Turbulent Jet in a Crossflow, Journal of the Hydraulics Division, Proc. of the ASCE, HY(6) (1967), 56-63.

Sherif, S. A. and Pletcher, R. H., Measurements of the Flow and Turbulence Characteristics of Round Jets in Crossflow, J. Fluids Engineering, 111 (1989), 165-171.

Yuan, L. L., Street, R. L. and Ferziger, J. H., Large Eddy Simulations of a Round Jet in Crossflow, J. Fluid Mech., 379 (1999), 71-104.

Author Profile

Kyung Chun Kim: He was educated at Pusan National University(B.A. 1979) and at Korea Advanced Institute of Science and Technology(M.S. 1981, Ph.D 1987) in Korea. His research interests are the identification of turbulence structures in complex flows, wind engineering and turbulent convective heat transfer using various types of experimental methods including PIV technique. He is a professor of school of mechanical engineering at Pusan National University, and director of the laboratory for Applied Fluid Mechanics in PNU.

Sang Ki Kim: He received his bachelor(1990) and master(1993) of engineering degrees in mechanical engineering from Pusan National University in Korea. He is currently pursuing a Ph.D under the supervision of Prof. K. C. Kim in the area of turbulent flow.

Sang Youl Yoon: He received his bachelor(1998) and master(2000) of engineering degrees in mechanical engineering from Pusan National University in Korea. He is currently pursuing a Ph.D under the supervision of Prof. K.C.Kim in the area of micro-fluidics.